

**Photoemission study of CO adsorption on ordered Pb/Ni (111) surface phases**

V. Matolín,\* I. Matolínová, N. Tsud, S. Fabík, and J. Libra

*Charles University, Faculty of Mathematics and Physics, Department of Electronics and Vacuum Physics, V Holešovičkách 2, 18000 Prague 8, Czech Republic*

V. Dudr and V. Cháb

*Institute of Physics, Academy of Sciences of the Czech Republic, Cukrovarnická 10, 16253 Prague 6, Czech Republic*

K. C. Prince

*Sincrotrone Trieste, Strada Statale 14, km 163.5, 34012 Basovizza-Trieste, Italy*

(Received 24 November 2005; revised manuscript received 29 May 2006; published 16 August 2006)

Pb/Ni (111) surface phases were investigated by synchrotron radiation photoemission and low-energy electron diffraction. For room temperature deposition of Pb, two surface ordered layers,  $(3 \times 3)$  and  $(4 \times 4)$ , were observed. The Pb  $5d$  and Pb  $4f$  core levels as well as valence band spectra indicated a weak chemical interaction between Pb and Ni, and the formation of a close-packed overlayer with Pb atoms in two different adsorption sites. Annealing of the Pb/Ni (111) surface led to the formation of the  $(\sqrt{3} \times \sqrt{3})R30^\circ$  reconstruction, characterized by a topmost layer consisting of a substitutional alloy. The transformation to the  $(\sqrt{3} \times \sqrt{3})R30^\circ$  structure was accompanied by the appearance of a strong photoelectron diffraction effect, confirming embedding of Pb atoms in the Ni(111) first surface layer. CO adsorption results showed that lead simply blocked the CO adsorption sites for the unannealed surface while the surface alloy exhibited a chemical effect of weakening of the CO-Ni bond. The Pb  $5d$  core-level shift indicated charge transfer from Pb to the surface, particularly for  $(4 \times 4)$  and  $(\sqrt{3} \times \sqrt{3})R30^\circ$  structures.

DOI: [10.1103/PhysRevB.74.075416](https://doi.org/10.1103/PhysRevB.74.075416)

PACS number(s): 82.45.Jn, 82.65.+r

**I. INTRODUCTION**

Metallic binary materials of nanometer dimensions may form phases and structures which have no corresponding bulk counterparts and which are affected by the interaction with the substrate and/or by the confinement to atomic dimensions. The consequence is that materials with novel properties can be obtained, which originate from artificial structuring, spatial confinement, and proximity effects of dissimilar materials, such as immiscible metals. The exploitation of such novel phases in the field of catalysts, particularly in CO oxidation on Pb-Ni surface alloy, is the general underlying goal of the present work.

During the last few years several studies have shown the structural variety of Pb/Ni (111) surface phases involving a strong modification of the effective radius of the Pb adsorbate atoms. Gürtler and Jacobi<sup>1,2</sup> and Umezawa *et al.*<sup>3</sup> used ultraviolet photoemission spectroscopy (UPS), low-energy electron diffraction (LEED), and ion scattering and showed that Pb deposited on Ni(111) at 300 K formed  $(3 \times 3)$  and  $(4 \times 4)$  structures. The  $(3 \times 3)$  surface phase was observed for 1 monolayer (ML) of Pb atoms forming a hexagonal close-packed (hcp) structure with a Pb-Pb atom spacing of 3.74 Å, corresponding to that of the bulk Pb(111) plane. A transition from the  $(3 \times 3)$  to the  $(4 \times 4)$  structure was observed after additional deposition of 0.2 ML and was interpreted as a compressed close-packed structure that was characterized by reduced Pb-Pb spacing and therefore a decrease of Pb atom radius.<sup>3</sup> UPS results<sup>1,2</sup> showed a Pb  $5d_{5/2}$  core level shift to higher binding energy with increasing lead coverage at room temperature. Krupski and coworkers<sup>4-6</sup> proposed a Pb/Ni (111) growth model for qualitatively different

systems composed of Pb multilayers that can be described as a twin interface with *abcBAC* sequence, i.e., Pb atom adsorption in the hcp position. Since their technique was not sensitive to the first atomic layer at the interface but only to the relative orientations of the substrate and overlayer, the twinning observed could equally well be interpreted as a sequence such as *abcACB*, i.e., Pb atoms in face-centered cubic (fcc) sites.

Annealing of the Pb-covered surface was found to give rise to a stable Ni(111)- $(\sqrt{3} \times \sqrt{3})R30^\circ$ -Pb surface phase,<sup>7</sup> with Pb atoms incorporated into the first Ni(111) layer and with a Pb atom outward displacement of 0.2 Å. The formation of a Ni(111)- $(\sqrt{3} \times \sqrt{3})R30^\circ$ -Pb substitutional alloy was confirmed in Ref. 8, and the Pb atoms were suggested to be in fcc sites. It was shown that in the alloy phase the Pb effective radius was 0.4 Å smaller than in bulk crystalline Pb. Tensor LEED analysis of the Ni(111)- $(\sqrt{3} \times \sqrt{3})R30^\circ$ -Pb surface<sup>9</sup> confirmed earlier findings of a strong reduction in the effective radius, which was attributed to the influence of surface valence electron charge smoothing and an associated surface stress effect. The amplitude of the surface alloy rumpling was found to be 0.73 Å.

Despite detailed studies of the Pb/Ni (111) surface phase structure, the chemical properties of such alloys remain unexplored. Alloys of metals with *d*- and *s,p*-valence electrons are generally characterized by a shift of the centroid of the *d*-electron binding energy away from the Fermi level accompanied by a decrease of surface reactivity, which can be manifested as a decrease of CO adsorption temperature.<sup>10-12</sup> Our recent study of Pb interaction with a Pd(110) crystal suggested that a major aspect of the Pb poisoning effect on CO oxidation of the Pd-containing catalysts was the reduction of the heat of CO adsorption.<sup>13</sup>

In the present work the formation of the Pb/Ni (111) interface and surface alloy formation were investigated by means of synchrotron radiation excited photoemission and LEED in the context of a study of surface structure, reactivity, and charge-transfer effects. As a reactivity test we selected the adsorption properties of CO, a commonly used molecule which is important in many reactions.

## II. EXPERIMENT

The experiments were performed at the Materials Science Beamline at the Elettra synchrotron light source in Trieste. It is a bending magnet beamline with a plane grating monochromator, based on the SX-700 concept.<sup>14</sup> The ultrahigh vacuum (UHV) experimental chamber is equipped with a 150 mm mean radius electron energy analyzer, rear-view LEED optics, a Pb evaporation source, and an ion gun. The base pressure of the vacuum chamber is  $1 \times 10^{-10}$  mbar.

The core-level spectra were recorded at normal emission of the photoelectrons with respect to the surface at two photon energies: 48.7 eV for the valence band and Pb 5*d* core levels and 400.6 eV for the Pb 4*f* and C 1*s* core levels. The total resolution (analyzer+photons+natural linewidth) was determined by measuring the width of the Fermi level at a temperature of 120 K and the values were 120 meV (50 eV) and 310 meV (400 eV). At this temperature the intrinsic width of the Fermi level is 33 meV. The photoelectron peak intensities were normalized to the incident photon flux.

The nickel crystal was a disk of 10 mm diameter and 1.5 mm thickness, oriented to within 0.2° of the (111) plane. Cleaning was performed by cycles of sputtering and flashing to 970 K until no contamination was detected by photoelectron spectroscopy at photon energies of 400 and 600 eV. The Pb metal was evaporated from a Knudsen cell onto the clean Ni(111) surface at 300 K.

## III. RESULTS

Pb was evaporated onto the Ni(111) surface at 300 K for fixed times and using a constant evaporation rate. The overlayer structure was monitored by LEED, and the (3×3) reconstruction formed after 5 min Pb deposition. After 7 min (3×3) spots appeared mixed with weak spots of the (4×4) structure, leading to a sharp (4×4) pattern after 8 min Pb deposition. We concluded that 6 min of Pb deposition corresponded to the formation of a complete (3×3) structure, i.e., to the formation of a monolayer with a coverage of 1 ML of lead,<sup>3</sup> and used this result to calibrate the evaporation time in terms of coverage. Annealing of the sample with a complete (3×3) structure at 820 K for several seconds and subsequent cooling to 300 K resulted in a sharp Ni(111)-(√3×√3)R30°-Pb structure. These results are in agreement with previously published experiments, according to which the (√3×√3)R30° structure corresponds to a substitutional alloy with Pb atoms embedded in the Ni(111) surface.<sup>3,4,7-9</sup>

The growth of the Pb overlayer on the Ni(111) surface was also investigated by means of photoelectron spectroscopy. The evolution of the valence band region and Pb 5*d*

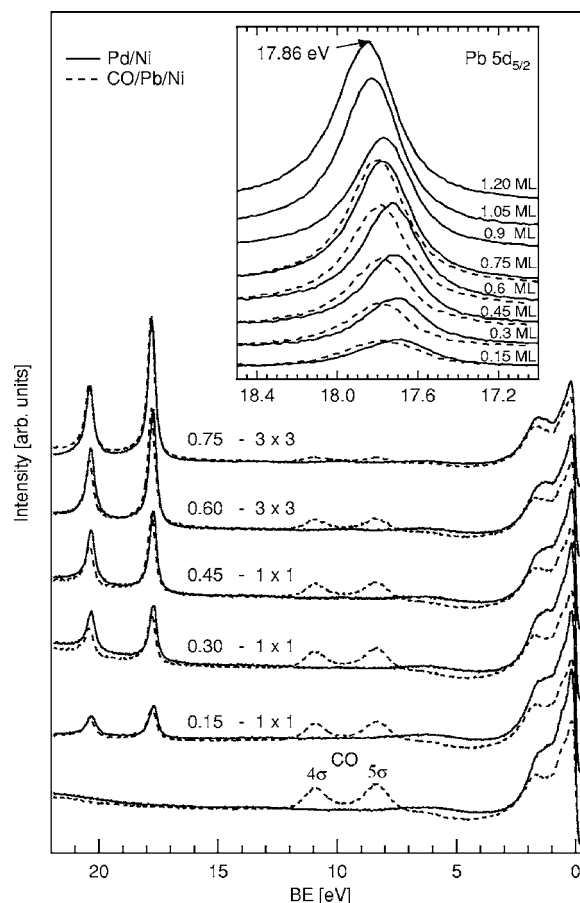


FIG. 1. Valence band and outer core levels (Pb 5*d*) for clean and CO-covered surfaces. Inset: Pb 5*d*<sub>5/2</sub> core level as a function of coverage.

core level was monitored at a photon energy of 48.7 eV, giving nearly maximum photoionization cross section for the Ni 3*d* and Pb 5*d* levels. Figure 1 shows the spectra as a function of lead coverage, and a sharp Pb 5*d* doublet appeared progressively. The Pb 5*d*<sub>5/2</sub> peak spectra are plotted in the inset of Fig. 1 for the coverage range from 0.15 to 1.2 ML. The binding energy (BE) of the Pb 5*d*<sub>5/2</sub> peak varied from 17.70 eV for 0.15 ML to 17.80 eV for 0.9 ML and then shifted to 17.86 eV for 1.05 and 1.2 ML, in agreement with earlier UPS study results.<sup>1,2</sup>

The Pb 5*d* BE shift can be explained by charge transfer from Pb atoms due to delocalization of the Pb 6*s*,*p* valence electrons over the Ni surface. We have observed similar shifts of the Pb 5*d* peak on a semiconducting surface due to charge fluctuations for the Pb/Si system.<sup>15</sup> The Ni 3*d* valence band exhibits a sharp Fermi edge for all deposits without a depletion of Ni states near the Fermi edge of the kind we observed for Pb adsorption on Pd(110).<sup>13</sup> The continuous decrease of the Ni 3*d* band intensity is caused by Ni signal attenuation due to Pb overlayer formation. CO adsorption was studied by measuring the valence band spectrum after 8 L ( $8 \times 10^{-6}$  Torr s) of CO exposure, to give saturation coverage on both clean and Pb-covered Ni(111) surfaces. In Fig. 1 we can see that three main features characterize CO adsorption on the Pb/Ni (111) surface: (i) appearance of peaks

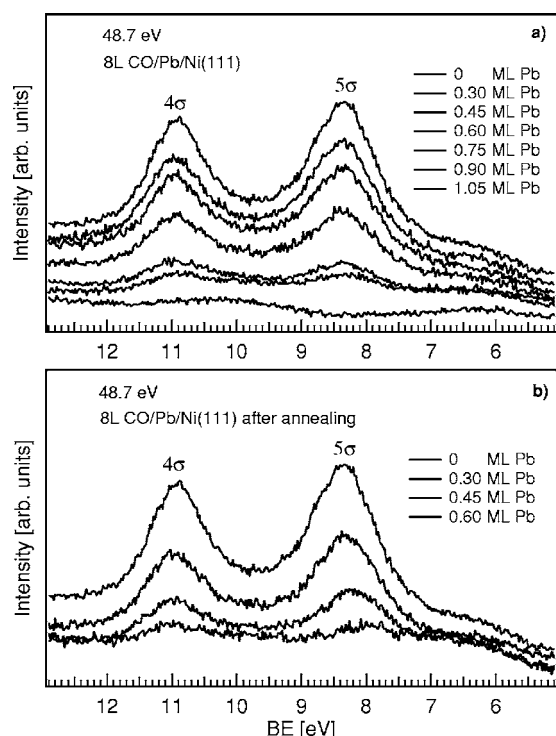


FIG. 2. CO molecular orbital spectra for different Pb coverages: (a) surface formed at 300 K and (b) surface annealed to 820 K.

due to  $4\sigma$  and  $5\sigma/1\pi$  CO molecular orbitals, (ii) depletion of Ni  $3d$  valence states, and (iii) shift of the Pb  $5d$  peak to higher BE. The CO molecular orbital spectra are presented in detail in Fig. 2(a), showing that the  $4\sigma$  and  $5\sigma/1\pi$  CO peaks at 11.0 and 8.4 eV peaks decreased in intensity with increasing Pb coverage. The sum of both molecular peak areas is plotted in Fig. 3, showing that the coverage of CO decreases linearly with Pb adsorption at 300 K and is negligible for 1 ML of Pb, which corresponds to the complete  $(3 \times 3)$  structure formation. This result is rather surprising because lead is generally considered as a strong catalyst poison with a potent inhibitor effect for CO adsorption. We can conclude that Pb atoms in this structure are simply blocking the

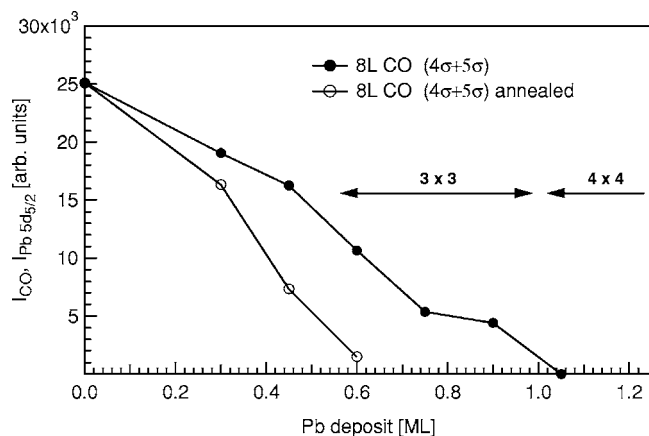


FIG. 3. CO molecular orbital intensity as a function of Pb coverage. Arrows indicate coverage intervals corresponding to  $(3 \times 3)$  and  $(4 \times 4)$  reconstructions observed by LEED.

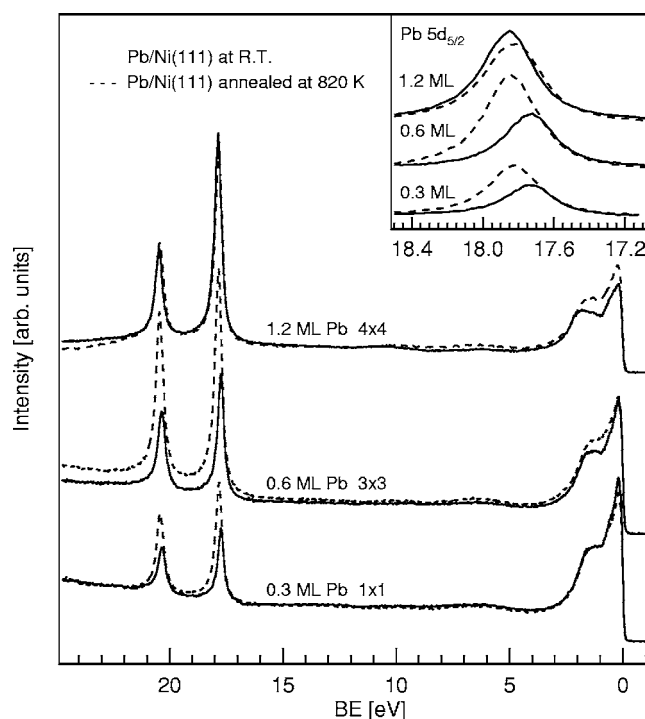


FIG. 4. Valence band and Pb  $5d$  spectra before and after annealing to 820 K. Inset: Pb  $5d_{5/2}$  peak.

Ni(111) surface without any long-range interaction with the CO molecules. The total disappearance of CO adsorption for 1 ML Pb coverage confirms a general assumption that CO is not bonded to Pb atoms, but nevertheless, a small shift of the Pb  $5d$  levels to higher BE can be seen in Fig. 1. The small Pb  $5d$  shift decreasing from 0.10 eV to 0.04 eV with increasing coverage, observed also in the case of Pb on Pd(110),<sup>13</sup> is assigned to CO adsorption on Ni atoms adjacent to Pb. The CO-Ni bond changes the electronic structure of the surface due to the Ni  $3d$ -CO  $2\pi^*$  charge donation that probably enhances a further charge transfer from Pb atoms to Ni.

Although the Pb-Ni system is an example of immiscible metals (Ni-Pb shows very limited solid solubility of Pb in Ni<sup>16</sup>), formation of the single-layer substitutional alloy of Ni<sub>2</sub>Pb stoichiometry can be activated by annealing the surface at 820 K.<sup>9</sup> In our experiment the Pb-Ni surface alloy was formed by annealing the Pb/Ni (111) substrate with lead coverages between 0.15 and 1.2 ML. Figure 4 shows valence band (VB) spectra for 0.3, 0.6, and 1.2 ML before and after annealing at 820 K. The spectra of the Pb  $5d$  levels show a rather surprising effect of a considerable enhancement of the peak intensity for coverages of 0.3 and 0.6 ML. The most likely explanation of this behavior is an increase of intensity due to photoelectron diffraction, linked to the surface phase transformation and embedding of Pb atoms into the first Ni layer. This effect cannot be caused by any out diffusion of lead atoms to the surface from the subsurface because we did not observe this behavior for Pb  $4f$  core level intensities measured at a photon energy of 400.6 eV (see Fig. 5). The angular dependence of this behavior is clearly seen in Fig. 6, which presents the intensity of the Pb  $5d_{5/2}$  core-level intensity at normal emission and  $60^\circ$  emission with respect to the

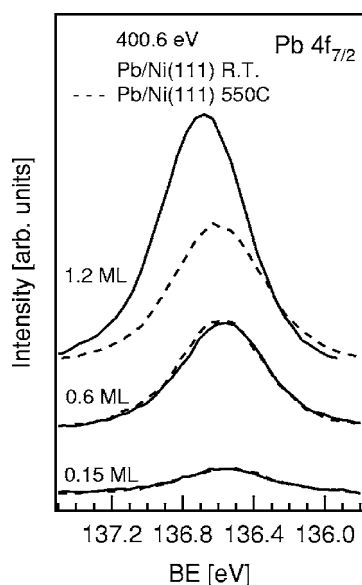


FIG. 5. Pb 4*f* core levels before and after annealing.

crystal normal along the  $\langle 112 \rangle$  azimuth. The hypothesis of diffraction effects is supported by cluster calculations using the EDAC software<sup>17</sup> that is discussed in more detail in the Discussion section.

The Pb 5*d*<sub>5/2</sub> spectra at different coverages are shown in the Fig. 4 inset. On annealing, the Pb 5*d*<sub>5/2</sub> peak shifts to a higher binding energy of 17.81 eV for 0.3 ML coverage and to 17.85 eV for 0.6 ML. This shift can be explained by charge transfer from Pb atoms to the Ni substrate, in agreement with the structural studies showing an effective radius reduction of the Pb atoms.<sup>9</sup> A similar shift can be seen for the as-deposited (4 × 4)-Pb structure (curve labeled 1.2 ML in Fig. 4). This finding is in good agreement with the ICISS study of the (3 × 3) → (4 × 4) structure transition<sup>3</sup> that is accompanied by a strong reduction of the Pb atomic radius to the value below the Pb nearest-neighbor distance in the bulk. The annealing leads to the (4 × 4) → (√3 × √3)R30° transition, i.e., to the conservation of reduced lead atomic size and

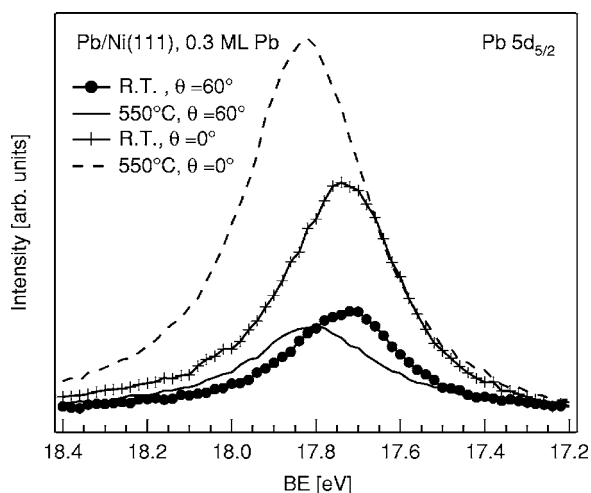


FIG. 6. Pb 5*d*<sub>5/2</sub> spectra before and after annealing for normal and 60° photoelectron emission.

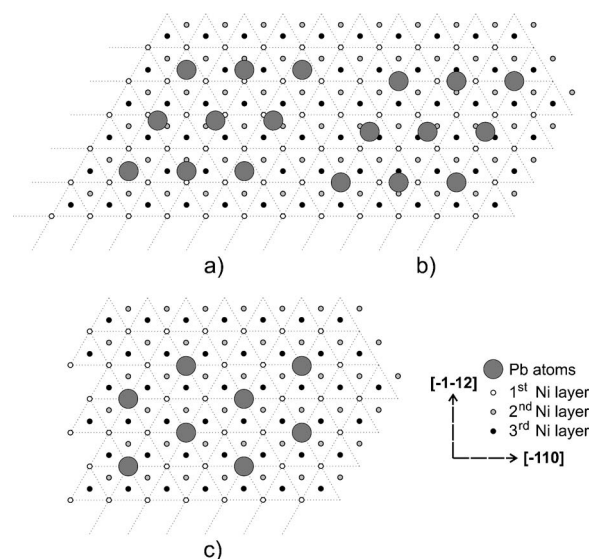


FIG. 7. Schematic diagrams of models of the observed Pb on Ni(111) structures: (a), (b) (3 × 3) overlayers, and (c) (√3 × √3)R30° reconstruction.

consequently to the conservation of the peak binding energy value. Thus, we can conclude that this photoelectron spectroscopy study confirmed the Pb-Ni charge transfer predicted from Pb atom radius reduction for both Ni(111)(4 × 4) and (√3 × √3)R30°-Pb structures.

Figure 5 shows the Pb 4*f*<sub>7/2</sub> core-level intensity variations for three different Pb deposits before and after annealing at 820 K. One can see that contrary to the Pb 5*d* peak intensity in Fig. 4, the annealing did not cause any intensity variations for low and medium Pb coverage and induced an intensity decrease for 1.2 ML coverage. This behavior can be explained by assuming conservation of Pb atom uptake for low coverage (and no strong photoelectron diffraction effects) and a partial desorption of excess lead atoms [relative to the complete (√3 × √3)R30° structure] at higher coverage.

The CO molecular orbital intensity obtained after exposing the annealed Pb/Ni (111) surfaces to 8 L of CO as a function of coverage of deposited Pb is shown in Fig. 2(b). We can see that in this case the CO uptake decreases more rapidly compared to that of the nonannealed surface, and no CO adsorbs for coverages above 0.6 ML of Pb on the Ni(111) surface.

#### IV. DISCUSSION

Structural studies reported in the literature show that lead grows on the Ni(111) surface by forming a (3 × 3) structure that completely covers the surface. The model suggested in Ref. 7 shows the close-packed Pb(111) overlayer with Pb-Pb atomic distance corresponding to that of bulk lead (Pb atomic radius of 1.75 Å). We propose two models, showing the most probable Pb atom position relative to the Ni(111) substrate in Fig. 7(a) and 7(b). One of the primitive (3 × 3) nets is composed of Pb atoms adsorbed either in (a) Ni high-symmetry fcc hollow sites, or (b) in atop positions.



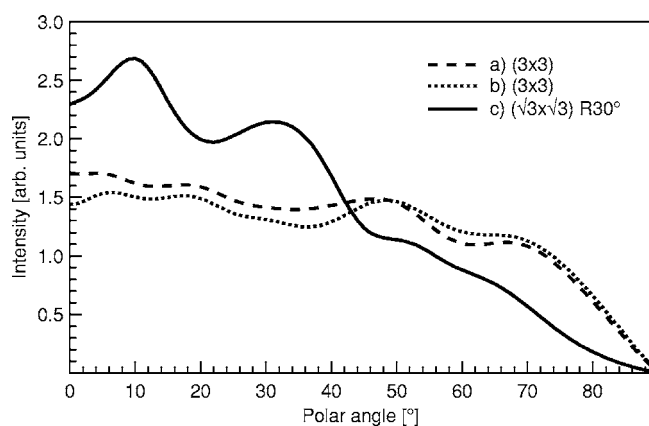


FIG. 8. The Pb  $5d_{5/2}$  intensity calculation vs photoelectron emission polar angle for  $\langle 112 \rangle$  azimuth for the structural models presented in Fig. 7.

Annealing the surface to 820 K leads to the  $(3 \times 3) \rightarrow (\sqrt{3} \times \sqrt{3})R30^\circ$  surface phase transition, Fig. 7(c), with the lead atoms occupying substitutional fcc sites to form a Pb-Ni surface alloy. The photoelectron diffraction intensity of the Pb  $5d$  level in the normal emission geometry is likely to be different in all three cases due to the Pb site symmetry difference. The Pb  $5d$  intensity was calculated using the EDAC software,<sup>17</sup> considering a hemispherical cluster composed of 700 Ni atoms in eight layers, and gave the results plotted as a polar intensity plot for the  $\langle 112 \rangle$  azimuthal direction in Fig. 8. The lead atoms in the substitutional fcc position [Fig. 7(c)] were fixed at an outward displacement of 0.7 Å (reported in Ref. 9). We compared the calculated and experimental intensities obtained for Pb adsorption sites indicated in Fig. 7(a)–7(c). The relative enhancement of the intensity corresponding to the  $(3 \times 3) \rightarrow (\sqrt{3} \times \sqrt{3})R30^\circ$  transition was obtained by integrating the angle-resolved intensities over the analyzer acceptance angle of  $8^\circ$  used for the measurement in both polar directions ( $\theta=0^\circ$  and  $60^\circ$ ). The obtained intensity increases for normal photoelectron emission were 1.4 (a) and 1.6 (b). We can see that the second calculated signal enhancement due to diffraction is in better agreement with the experimental value in Fig. 4, 1.6. In addition, good agreement between calculated and experimental values is obtained for a polar angle of  $60^\circ$ , both indicating a small intensity decrease due to the  $(3 \times 3) \rightarrow (\sqrt{3} \times \sqrt{3})R30^\circ$  transition: 0.71 [calculated (a)], 0.74 [calculated (b)], and 0.80 (experiment). Therefore we conclude that the Pb  $5d$  intensity enhancement is due to diffraction and the Pb  $(3 \times 3)$  structure presented in Fig. 7(b) with Pb atoms in atop and bridge positions is more likely.

For all coverages the Pb  $5d_{5/2}$  peaks can be fitted with a convolution of Lorentzian and Gaussian lines of 0.3 and 0.1 eV width. In Fig. 1 (inset) we can see that during overlayer growth the BE is constant at a value of 17.70 eV below 0.3 ML, corresponding to that of metallic lead. Above 0.3 ML the BE increases to 17.79 eV. The origin of this BE shift is not clear, but it can be explained, in agreement with the proposed structural model, by a surface phase transition accompanying the completion of the  $(3 \times 3)$  structure. One scenario could be adsorption of Pb atoms in high-symmetry

hollow sites and their subsequent movement to bridge and atop positions (model b in Fig. 7). In order to answer this question, an investigation of the Ni(111)-Pb( $3 \times 3$ ) overlayer local structure using dynamic LEED and XPD methods will be necessary.

In Fig. 4 we can see that the BE increases further with the formation of the  $(4 \times 4)$  structure. This increase could be explained by charge transfer from Pb atoms, accompanying their radius reduction.<sup>3</sup>

Annealing of the Pb/Ni (111) overlayers leads to the BE shift shown in Figs. 4 and 6. As we mentioned in the previous section, the Pb  $5d_{5/2}$  peak shifts to a higher binding energy of 17.81 eV for 0.3 ML coverage, and to 17.85 eV for 0.6 ML. Because of the large difference between the covalent radii of Ni and Pb atoms, the process of Pb atom movement into substitutional fcc sites is driven by the tendency to decrease the surface corrugation that is accompanied by a strong reduction in Pb atom effective radius<sup>9</sup> and consequently, by surface charge redistribution. Accordingly, the BE shift can be explained by the charge transfer from Pb atoms to the Ni substrate (BE increase) that can be expected in the case of the reduction of the effective radius of the Pb atoms.

Turning now to the CO adsorption experiments, CO molecules have been found to adsorb on clean Ni(111) surfaces in all sites: hollow, bridge, and atop positions,<sup>18–21</sup> depending on adsorption conditions (coverage, temperature). We recall that on metal surfaces, the  $5\sigma$ - $4\sigma$  molecular orbital separation (the  $5\sigma$  overlaps the  $1\pi$ ) decreases significantly with increasing CO adsorption energy.<sup>22,23</sup> In our experiment both these CO molecular orbitals had constant BE values when CO was coadsorbed with Pb deposited at 300 K (8.4 and 11.0 eV), as can be seen in Fig. 2(a), with an energy difference  $\Delta=2.6$  eV. We conclude that there is at most a negligible chemical effect influencing the CO adsorption for  $(3 \times 3)$  reconstructions. This is consistent with a linear decrease of the CO uptake with increasing Pb coverage in Fig. 3 so that the Pb atoms simply block the adsorption of CO. This is quite a different situation from that of the Pb/Pd (110)<sup>13</sup> system, where we observed strong Pb-Pd interaction at 300 K [the  $5\sigma$ - $4\sigma$  separation was 3.6 eV for the  $c(2 \times 2)$  reconstruction and 2.7 eV for clean Pd(110)] that was accompanied by a decrease of CO desorption temperature.

Contrary to this result for the  $(3 \times 3)$  reconstruction, for the annealed surface we observed an orbital energy difference of  $\Delta=2.6$  eV for 0.3 ML of Pb, and an increasing shift of the  $5\sigma$  level to lower BE to  $\Delta=3.1$  eV for 0.6 ML, indicating weakening of the CO-Ni bond. So in this case the poisoning effect is due to the formation of a less reactive surface, compared with the pure Ni(111) surface, that is in agreement with the observed formation of the surface substitutional Pb-Ni alloy.

We conjecture that this difference between Ni and Pd occurs because the Ni  $3d$  orbitals are more compact than the Pd  $4d$  orbitals, reducing the overlap with the Pb  $sp$  orbitals. This affects not only the surface but also the bulk properties: Ni does not form intermetallic compounds with Pb, while Pd does. The Ni surface is not strongly alloyed in the  $(3 \times 3)$  structure, and its chemical interaction with CO is also unaf-

fect. Conversely, in the  $(\sqrt{3} \times \sqrt{3})R30^\circ$  structure a surface alloy is formed (which is not possible in the bulk), and the chemical properties also change significantly.

Another surprising difference between Ni and Pd is that the density of states at the top of the valence band is not strongly affected upon alloy formation. As mentioned in the Introduction, the usual model for the decrease in reactivity of a transition metal catalyst by a poison is that the centroid of the density of  $d$  states moves to higher binding energy. In the present case we have a decrease in reactivity without the expected change in the density of states.

## V. CONCLUSIONS

High-resolution synchrotron radiation photoelectron spectroscopy and LEED were used to study the growth of Pb overlayers on the Ni(111) surface at 300 K, at which temperature  $(3 \times 3)$  and  $(4 \times 4)$  superstructures form. A structural model of the  $(3 \times 3)$  reconstruction consisting of a close packed Pb/Ni (111) interface was developed. We proposed a corrugated structure formed by two types of Pb atom adsorption sites—the atop and bridge positions. Spectra after CO adsorption showed that lead atoms inhibited CO adsorption in a purely geometrical way by site blocking on the Ni surface, with negligible Pb-Ni interaction. The formation of the  $(4 \times 4)$  structure, that is accompanied by Pb overlayer compression and Pb atom effective radius reduction,<sup>3</sup> caused an additional Pb  $5d$  level shift.

Surface annealing producing the  $(3 \times 3) \rightarrow (\sqrt{3} \times \sqrt{3})R30^\circ$  transition was accompanied by a strong photoelectron diffraction effect in normal emission, causing an enhancement of the Pb  $5d$  core-level intensity. Diffraction intensity calculations showed that this was consistent with our  $(3 \times 3)$  structural model and the  $(\sqrt{3} \times \sqrt{3})R30^\circ$  reconstruction structure proposed in Refs. 7–9 i.e., the Pb atoms moving to substitutional fcc sites. The Pb  $5d$  core level shift was consistent with the charge transfer that must accompany the Pb radius reduction. The  $(\sqrt{3} \times \sqrt{3})R30^\circ$  surface alloy showed a weakening of the Ni-CO bond measured from the  $5\sigma$ - $4\sigma$  molecular orbital separation. This result can be considered as a striking example of the flexibility of poisoning effects in carbon monoxide catalysis, showing a structure-dependent influence of bimetallic surface formation on CO-metal bond strength.

This spectroscopic study extends previous discussions<sup>3,4,7-9</sup> on the structural transformations of the Pb-Ni (111) phase.

## ACKNOWLEDGMENTS

The Materials Science Beamline is supported by the Ministry of Education of the Czech Republic under Grant No. INGO LA 151 and by Charles University under Grant No. GAUK 303/2004. This work is a part of the research program No. MSM 0021620834 that is financed by the Ministry of Education of the Czech Republic.

\*Corresponding author.

Electronic address: matolin@mbox.troja.mff.cuni.cz

- <sup>1</sup>K. Gärtler and K. Jacobi, Surf. Sci. **134**, 309 (1983).
- <sup>2</sup>K. Gärtler and K. Jacobi, Surf. Sci. **152/153**, 272 (1985).
- <sup>3</sup>K. Umezawa, A. Takahashi, T. Yumura, S. Nakanishi, and W. M. Gibson, Surf. Sci. **365**, 118 (1996).
- <sup>4</sup>A. Krupski and S. Mroz, Phys. Rev. B **66**, 035410 (2002).
- <sup>5</sup>A. Krupski and M. Nowicki, Surf. Sci. **575**, 147 (2005).
- <sup>6</sup>A. Krupski, Phys. Rev. B **B72**, 125426 (2005).
- <sup>7</sup>K. Umezawa, S. Nakanishi, T. Yumura, W. M. Gibson, M. Watanabe, Y. Kido, S. Yamamoto, Y. Aoki, and H. Naramoto, Phys. Rev. B **56**, 10585 (1997).
- <sup>8</sup>D. Brown, P. D. Quinn, D. P. Woodruff, P. Bailey, and T. C. Q. Noakes, Phys. Rev. B **61**, 7706 (2000).
- <sup>9</sup>P. D. Quinn, C. Bittencourt, and D. P. Woodruff, Phys. Rev. B **65**, 233404 (2002).
- <sup>10</sup>V. Matolín, I. Stará, N. Tsud, and V. Johánek, Prog. Surf. Sci. **67**, 167 (2001).
- <sup>11</sup>N. Tsud, V. Johánek, I. Stará, K. Veltruská, and V. Matolín, Thin Solid Films **391**, 204 (2001).
- <sup>12</sup>V. Matolín, I. Matolínová, F. Šutara, and K. Veltruská, Surf. Sci. **566-568**, 1093 (2004).
- <sup>13</sup>N. Tsud, V. Dudr, S. Fabík, C. Brun, V. Cháb, V. Matolín, and K.

C. Prince, Surf. Sci. **560**, 259 (2004).

- <sup>14</sup>R. Vašina, V. Kolařík, P. Doležel, M. Mynář, M. Vondráček, V. Cháb, J. Slezák, C. Comicioli, and K. C. Prince, Nucl. Instrum. Methods Phys. Res. A **467-468**, 561 (2001).
- <sup>15</sup>V. Dudr, N. Tsud, S. Fabík, M. Vondráček, V. Matolín, V. Cháb, and K. C. Prince, Phys. Rev. B **70**, 155334 (2004).
- <sup>16</sup>*Binary Alloy Phase Diagrams*, 2nd ed., edited by T. B. Massalski (ASM International, Metals Park, OH, 1990).
- <sup>17</sup>F. J. García de Abajo, M. A. Van Hove, and C. S. Fadley, Phys. Rev. B **63**, 075404 (2001).
- <sup>18</sup>P. M. Williams, P. Buchter, J. Wood, and K. Jacobi, Phys. Rev. B **14**, 3215 (1976).
- <sup>19</sup>S. L. Tang, M. B. Lee, Q. Y. Yang, J. D. Beckerle, and S. T. Ceyer, J. Chem. Phys. **84**, 1876 (1986).
- <sup>20</sup>A. Bandara, S. Katano, J. Kubota, K. Onda, A. Wada, K. Domen, and C. Hirose, Chem. Phys. Lett. **290**, 261 (1998).
- <sup>21</sup>S. Masuda, R. Suzuki, M. Aoki, Y. Morikawa, R. Kishi, and M. Kawai, J. Chem. Phys. **114**, 8546 (2001).
- <sup>22</sup>R. Miranda, K. Wandelt, D. Rieger, and R. D. Schnell, Surf. Sci. **139**, 430 (1984).
- <sup>23</sup>J. Kandler, B. Elteter, H. Busse, G. R. Castro, and K. Wandelt, Surf. Sci. **331-333**, 18 (1995).